

Melting of vortex lattice in magnetic superconductor RbEuFe₄As₄

A. E. Koshelev,¹ K. Willa,^{1,2} R. Willa,^{1,3} M. P. Smylie,^{1,4} J.-K. Bao,¹
D. Y. Chung,¹ M. G. Kanatzidis,^{1,5} W.-K. Kwok,¹ and U. Welp¹

¹*Materials Science Division, Argonne National Laboratory,
9700 South Cass Avenue, Lemont, IL 60439, USA*

²*Institute for Solid-State Physics, Karlsruhe Institute of Technology, 76021 Karlsruhe, Germany*

³*Institute for Theory of Condensed Matter, Karlsruhe Institute of Technology, 76131 Karlsruhe, Germany*

⁴*Department of Physics and Astronomy, Hofstra University, Hempstead, New York 11549*

⁵*Department of Chemistry, Northwestern University, Evanston, Illinois, 60208, USA*

(Dated: August 26, 2019)

The iron-based superconductors are characterized by strong fluctuations due to high transition temperatures and small coherence lengths. We investigate fluctuation behavior in the magnetic ironpnictide superconductor RbEuFe₄As₄ by calorimetry and transport. We find that the broadening of the specific-heat transition in magnetic fields is very well described by the lowest-Landau-level scaling. We report calorimetric and transport observations for vortex-lattice melting, which is seen as a sharp drop of the resistivity and a step of the specific heat at the magnetic-field-dependent temperature. The melting line in the temperature/magnetic-field plane lies noticeably below the upper-critical-field line and its location is in quantitative agreement with theoretical predictions without fitting parameters. Finally, we compare the melting behavior of RbEuFe₄As₄ with other superconducting materials showing that thermal fluctuations of vortices are not as prevalent as in the high-temperature superconducting cuprates, yet they still noticeably influence the properties of the vortex matter.

I. INTRODUCTION

Mean-field theory of type II superconductors predicts the formation of a periodic vortex lattice as a result of a continuous phase transition from the normal state at the upper critical field [1]. Thermal fluctuations qualitatively modify this scenario [2]. The upper critical field becomes a crossover separating the normal phase from the vortex liquid state. This intermediate vortex liquid freezes into the lattice state via a first-order transition and the corresponding vortex-lattice melting field lies below the upper critical field.

The extent of the vortex-liquid region varies widely between different superconducting materials and depends on the strength of thermal fluctuations, quantitatively characterized by the Ginzburg-Levanyuk number, Gi [2–4]. This number is uniquely determined by the superconducting parameters as

$$Gi = \frac{1}{2} \left(\frac{8\pi^2 \lambda_{ab0}^2 T_c}{\Phi_0^2 \xi_{c0}} \right)^2. \quad (1)$$

Here and below ξ_{ab0} and ξ_{c0} are the coherence lengths and λ_{ab0} and λ_{c0} are the London penetration depths¹. At temperature $T - T_c \sim Gi T_c$ the fluctuation contribution to the specific heat is approximately equal to the specific-heat jump at the superconducting transition. The magnetic field increases the fluctuation width of the transition. In the field range $B > Gi B'_{c2} T_c$,

the fluctuation broadening is determined by the field-dependent Ginzburg-Levanyuk number [2], $Gi(B) = Gi^{1/3} [B/(B'_{c2} T_c)]^{2/3}$, where $B'_{c2} = |dB_{c2}/dT|$ is the linear slope of the upper critical field at T_c . The Ginzburg-Levanyuk numbers for several representative superconducting materials are summarized in Table I. In conventional type-II superconductors the Ginzburg-Levanyuk number is very small (e.g. for niobium $Gi \approx 7 \cdot 10^{-12}$), and the vortex liquid occupies only a tiny and hard-to-detect strip below the upper critical field.

Soon after the discovery of the cuprate high-temperature superconductors, it became clear that the Ginzburg-Levanyuk number in these materials is exceptionally large, $\sim 10^{-3}$ - 10^{-2} , due to their very high transition temperatures, small coherence lengths and large anisotropies. Early theoretical estimates based on the Lindemann criterion [14] suggested that the melting magnetic field is significantly lower than the upper critical field and the vortex liquid state occupies a substantial portion of the temperature-field phase diagram. The transport measurements performed on high-quality YBa₂Cu₃O_{7- δ} (YBCO) single crystals showed that the resistivity sharply drops to zero from a finite value at the field-dependent temperature $T_m(B)$ [15–17], which was interpreted as a manifestation of the first-order melting transition. Later thermodynamic measurements have convincingly supported this interpretation: it was demonstrated that the magnetization features a small step [12, 18, 19] while the specific heat has a peak and a step at the transition point [13, 20, 21].

The magnetic field at which melting occurs in YBCO is typically one quarter of the upper critical field, i.e., even though the melting is well separated from the mean-field crossover, it occurs at a comparable magnetic field

¹ In quantitative estimates for Gi , we take the Ginzburg-Landau values for the coherence length and the London penetration depth rather than their low-temperature values.

	Nb	Nb ₃ Sn	SnMo ₆ S ₈	RbEuFe ₄ As ₄	FeSe	YBa ₂ Cu ₃ O ₇
Refs.	[5, 6]	[7]	[8]	[9, 10]	[11]	[12, 13]
T_c [K]	9.25	18	14.2	36.5	9.1	93.7
B'_{c2} [T/K]	0.044	1.6	2.9	4.2	3.2	1.8
γ	1	1	1	1.7	4	7.8
ΔC [kJ/K·m ³]	13	55	22	59	3.3	42
ξ_{ab0} [nm]	28.6	3.4	2.8	1.46	3.4	1.4
λ_{ab0} [nm]	21.3	61.7	133	98	357	75
Gi	$6.9 \cdot 10^{-12}$	$1.3 \cdot 10^{-7}$	$2.5 \cdot 10^{-6}$	$5.3 \cdot 10^{-5}$	$6.1 \cdot 10^{-4}$	$2 \cdot 10^{-3}$

TABLE I. Superconducting parameters and the corresponding Ginzburg-Levanyuk numbers, Eq. (1), for several materials. Here ξ_{ab0} and λ_{ab0} are the Ginzburg-Landau values of the coherence length and London penetration depth. The former is extracted from the linear slope of the upper critical field, $\xi_{ab0} = \sqrt{\Phi_0/2\pi T_c B'_{c2}}$ with $B'_{c2} \equiv dB_{c2,c}/dT$ for $T \rightarrow T_c$, while the latter is extracted from the specific heat jump, $\lambda_{ab0} = \Phi_0 / (4\pi \xi_{ab0} \sqrt{2\pi \Delta C T_c})$. γ is the anisotropy of the upper critical field.

strength. Consequently, the liquid and crystal state occupy comparable fractions of the vortex-matter phase space. This situation is different in the much more anisotropic cuprate Bi₂Sr₂CaCu₂O_{8- δ} (BSCCO), which represents an extreme scenario. The maximum melting field in this compound typically ranges from 300 G for optimal doping to 800 G in overdoped samples [22–24]. This is several thousand times smaller than the upper critical field ($\sim 100 - 200$ T) meaning that the liquid state occupies most of the vortex-matter region in the temperature-magnetic field phase diagram. Such low melting fields allowed for direct monitoring of the crystalline long-range order across the transition by techniques sensitive to magnetic-field contrast, among which are neutron scattering [25], muon spin rotation [26], and direct scanning Hall-probe imaging [27]. In addition, due to its first-order character, the melting transition is accompanied by the noticeable magnetization jump [28–30]. The observation of the first-order transition via the magnetization jump has been also reported for the compound (La_{1- x} Sr _{x})₂CuO₄ (LSCO) [31]. Depending on the doping level, the anisotropy factor of this compound varies between 20 and 50 situating this cuprate’s fluctuation strength between that of YBCO and BSCCO.

Extensive investigation of the vortex-lattice melting in high-temperature cuprates motivated more careful examination of this phenomenon in conventional superconductors. Specific-heat features associated with melting were reported for Nb₃Sn [7, 32] and the Chevrel phase SnMo₆S₈ [8]. Even though these isotropic materials are characterized by high transition temperatures (18 K for Nb₃Sn and 14.2 K for SnMo₆S₈) and upper critical fields (~ 29 T for Nb₃Sn and > 25 T for SnMo₆S₈), the melting field still is located very close to the upper critical field and the vortex liquid occupies a very small fraction of the vortex-matter phase space. In general, observation of the melting transition in any material requires high-quality uniform single crystals. A small amount of disorder is sufficient to transform the first-order transition into the continuous glass transition.

In terms of thermal fluctuations, iron pnictides are situated in between cuprates and conventional superconductors. In particular, the 122 and 1144 compounds—named after their chemical composition AFe₂As₂ [33–35], and ABFe₄As₄ [36] respectively—have transition temperatures above 30 K, c -axis upper critical fields reaching 80 T, Ginzburg-Landau parameter $\kappa = \lambda_{ab}/\xi_{ab} \approx 70$, and a relatively small superconducting anisotropy 1.5 – 2.5 [37–40]. These parameters combine to provide a Ginzburg-Levanyuk number $Gi \approx 5 \cdot 10^{-5} - 2 \cdot 10^{-4}$, of intermediate magnitude. One of the fluctuation effects observed in 122 compounds is a noticeable diamagnetic response above the superconducting transition in finite magnetic fields [41]. The observation of the vortex-lattice melting has been reported in Ba_{0.5}K_{0.5}Fe₂As₂ [42] using specific heat, thermal expansion, and magnetization measurements. In calorimetry, the transition has been seen as a small step in the temperature-dependent specific heat and a small peak develops at magnetic fields above 10 T. In the temperature range 29 – 33 K the melting field is approximately half of the upper critical field.

The recently discovered magnetically ordered iron-pnictide superconductor RbEuFe₄As₄ [9, 10, 43–46] has a transition temperature of 36.8 K and slopes of the upper critical field 4.2 T/K and 7 T/K for the c -axis and ab -plane direction, respectively [9, 10]. This compound also represents a rare case of magnetism coexisting with superconductivity. In fact, long-range magnetic order of Eu²⁺ magnetic moments develops below 15K without apparent suppression of superconductivity. In this paper, we report resistive and calorimetric observations of the vortex-lattice melting in single crystals of this material. We show that the melting transition reveals itself through an abrupt drop of the resistivity and a step in the specific heat at the field-dependent temperature $T_m(B)$. The location of the melting line in the phase diagram is similar to that of Ba_{0.5}K_{0.5}Fe₂As₂. We compare the transition line with the theoretical predictions using experimental parameters of the material and find quantitative agreement without fitting parameters.

II. THEORETICAL BACKGROUND

A. Lowest-Landau level scaling of specific heat

The shape of the superconducting order parameter near the upper critical field within mean-field theory is given by the lowest-Landau level (LLL) wave function for a particle with charge $2e$ [1]. At high magnetic field $B \gg GiB'_c T_c$ the fluctuating order parameter near the mean-field transition can be well approximated as a linear combination of LLL wave functions, while contributions from higher Landau levels can be treated within Gaussian approximation. In this LLL regime, the fluctuation width of the transition is determined by the field-dependent Ginzburg number $Gi(B)$ and increases proportionally to $B^{2/3}$.

Theoretical considerations [47–51] predict that within LLL regime, the superconducting contribution to the specific heat $C(B, T) - C_n(B, T)$ divided by the mean-field superconducting specific heat $C_{MF}(T)$ has to be a universal function of a single scaling parameter

$$a_T = r_{sc} \frac{T - T_{c2}(B)}{(BT)^{2/3}} \quad (2)$$

with the coefficient

$$r_{sc} = \left(\frac{B'_c \sqrt{2T_c}}{\sqrt{Gi}} \right)^{2/3}, \quad (3)$$

and $T_{c2}(B) = T_c - B/B'_c$ the mean-field transition temperature at fixed magnetic field B . This parameter corresponds to a shift of the temperature with respect to the mean-field transition normalized to the fluctuation broadening, $a_T \approx (T - T_{c2}(B))/Gi(B)T_{c2}(B)$. The scaling property implies that the experimental specific heat in the vicinity of the mean-field transition $T_{c2}(B)$ can be represented as

$$C(B, T) = C_n(B, T) + C_{MF}(T) c_{sc} \left[r_{sc} \frac{T - T_{c2}(B)}{(BT)^{2/3}} \right]. \quad (4)$$

The scaling function $c_{sc}(a_T)$ in this equation captures the strongest temperature dependence near $T_{c2}(B)$, while all smooth contributions can be absorbed into the normal and superconducting backgrounds. Its precise shape follows from the corresponding free-energy scaling function that has been computed in Refs. [50, 52].

B. Vortex-lattice melting

The dependence of the melting magnetic field of the vortex lattice on parameters of superconductors and temperature has been quantitatively investigated in two regimes. At high fields, close to the upper critical field, $H_{c2}(T)$, one can use the lowest Landau level (LLL) approximation. In this regime, the melting transition has

been studied by Monte-Carlo simulations [53] and analytically, using an elaborated evaluation of the free energies of the liquid and crystal states [51, 52]. At low magnetic fields, in the London regime [$B \ll H_{c2}(T)$], the vortex-lattice melting was investigated by Monte-Carlo simulations of the model of interacting lines [54] and the uniformly-frustrated XY model [55]. It was also demonstrated that these two approaches give consistent results [56].

The melting criterion in the LLL regime derived in Ref. [52] is²

$$a_T = -9.5 \quad (5)$$

where the parameter a_T is defined by Eqs. (2) and (3). For easier comparison with the low-field regime, we rewrite the criterion (5) as

$$\left(\frac{0.137 \varepsilon_0 \xi_c}{b_m T} \right)^2 (1 - b_m)^3 = 1 \quad (6)$$

with the c -axis coherence length $\xi_c(T)$, the reduced field $b_m = B_m(T)/H_{c2}(T)$, and the vortex line-energy scale $\varepsilon_0 = [\Phi_0/4\pi\lambda_{ab}(T)]^2$. Note that although the LLL regime is only justified for $1 - b_m \ll 1$, it usually works well beyond this range, i.e., at lower fields. Nevertheless, we point that this equation fails at describing the low-field behavior correctly, $b_m \ll 1$. In the London limit, $B \ll H_{c2}(T)$, the melting field rather reads $B_m \approx \Phi_0[0.1\varepsilon_0/(T\gamma)]^2$ [56] or

$$b_m \approx \left(\frac{\varepsilon_0 \xi_c}{4T} \right)^2. \quad (7)$$

Comparing this result with the LLL one in Eq. (6), we can introduce the interpolation formula

$$\left[\frac{\varepsilon_0 \xi_c (1 - 0.46b_m)}{4T} \right]^2 (1 - b_m)^3 = b_m. \quad (8)$$

Assuming the mean-field temperature dependences, $\varepsilon_0 = \varepsilon_{00}(1 - t)$ and $\xi_c = \xi_{c0}(1 - t)^{-1/2}$ with $t = T/T_c$, and the relation $Gi = (T_c/\xi_{c0}\varepsilon_{00})^2/8$ following from Eq. (1), we can represent the above equation in the form

$$\frac{(1 - 0.46b_m)(1 - b_m)^{3/2}}{8\sqrt{2b_m}} = \frac{\sqrt{Gi}t}{\sqrt{1 - t}}. \quad (9)$$

Here the parameter $t_{\text{eff}} \equiv t\sqrt{Gi/(1 - t)}$ on the right-hand side may be interpreted as an effective temperature, which determines the strength of thermal fluctuations. The solution of this equation provides the reduced

² This result also can be approximately expressed via the field dependent Ginzburg-Levanyuk number as $(T_{c2} - T_m)/T_{c2} = 7.57 Gi(B)$, where T_{c2} and T_m are the upper critical and melting temperatures at fixed field.

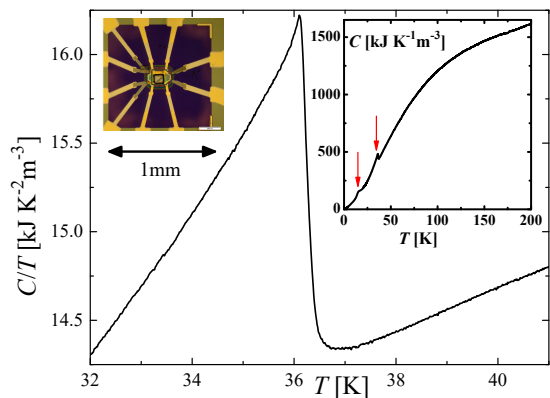


FIG. 1. Specific heat over temperature of a $\text{RbEuFe}_4\text{As}_4$ single crystal at the superconducting transition at 36.5K in zero field. The inset shows the specific heat during cooldown from high temperatures. The superconducting and the magnetic transitions are marked by the arrows. The picture in the upper left corner shows a microscope image of the measured crystal on the nanocalorimeter platform.

melting field in the wide range $H_{c1} \ll B_m < H_{c2}$. It does not apply to describe the region of extremely low fields, where the distance between the vortex lines becomes comparable to $\lambda_{ab}(T)$. In addition, the mean-field approximation assumed in Eq. (9) breaks down in the region of strong fluctuations, $1 - t < Gi$, where the critical 3D XY behavior develops.

III. EXPERIMENTAL DETAILS

Single crystals of $\text{RbEuFe}_4\text{As}_4$ were grown in RbAs flux, as described in Ref. [44]. For specific heat measurements, we mounted small ($100\mu\text{m} \times 100\mu\text{m} \times 10\mu\text{m}$), uncut, platelet-shaped single crystals onto a SiN membrane based nanocalorimeter platform [57, 58] using Apiezon grease. The probe was then inserted into a three-axis vector magnet (1T-1T-9T), where we estimate the field to be aligned with the crystal axes up to ± 3 degrees. The orientation of the specific heat platform could be changed from perpendicular to parallel to the 9T z -axis of the magnet. The specific heat was obtained from ac measurements ($f = 1\text{Hz}$ and $\delta T \sim 0.1\text{K}$) and the signal was recorded with a Synkrex lock-in amplifier. Resistivity samples were prepared by cutting larger $\text{RbEuFe}_4\text{As}_4$ crystals into bars and attaching 4 wires with Silver Epoxy. Then they were mounted into the same three-axis cryostat. The resistivity was then measured in a 4-point configuration at a constant current of 0.1mA. The data presented here is consistent with heat capacity and resistivity data published earlier in Refs. [9, 10].

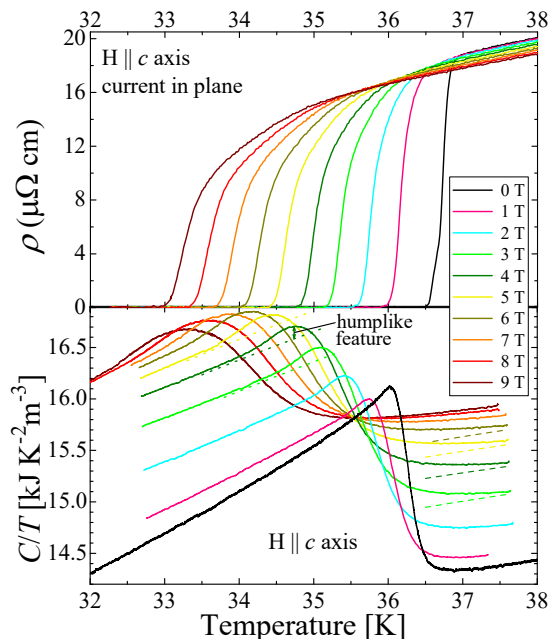


FIG. 2. *Top*: In plane resistivity for various magnetic fields along the c -axis for another $\text{RbEuFe}_4\text{As}_4$ single crystal. *Bottom*: Superconducting transition of $\text{RbEuFe}_4\text{As}_4$ as seen in specific heat with c -axis magnetic fields up to 9T. The transition broadens and shifts to lower temperatures with increasing field. The hump visible on the low-temperature side of the transition is taken as an indication for vortex lattice melting. The dotted and dashed lines in the lower plot show the representative superconducting mean-field and normal backgrounds, respectively, extracted from the scaling analysis, see text.

IV. RESULTS AND DISCUSSION

The zero-field superconducting transition of a $\text{RbEuFe}_4\text{As}_4$ single crystal as seen in specific heat is shown in Fig. 1. The specific-heat jump at the transition amounts to $\Delta C/T_c = 1.65 \pm 0.05 \text{ kJ/K}^2 \text{ m}^3$ ³. A noticeable upturn below the transition indicates that the broadening is caused by thermal fluctuations. The calorimetry data recorded at finite magnetic fields parallel to the c -axis, see Fig. 2(bottom), reveal a suppression of the transition temperature and a considerable broadening with increasing field strength. Additionally, a hump-like feature below the transition temperature is a characteristic indicator of entropy excess associated with the vortex liquid state. The vertical shift of the C/T curves are caused by the magnetic contribution to the specific heat

³ In this paper, we use volume specific heat in units of J/K m^3 , because it is this quantity that enters in all thermodynamic relations for superconductors. On the other hand, in experimental papers the molar specific heat in units of J/K mol is usually presented. The conversion can be done using the molar volume which for $\text{RbEuFe}_4\text{As}_4$ is approximately equal to $120.5 \text{ cm}^3/\text{mol}$.

arising from magnetic fluctuations of the Eu^{2+} moments, as discussed in Ref. [10].

We find that the broadening of the specific-heat transition with the increasing magnetic field is in excellent agreement with theoretical predictions for an intrinsic fluctuation mechanism. Figure 3 shows the LLL scaling plot of the specific heat in high magnetic fields, as suggested by Eq. (4). The theoretical scaling function shown in the figure is based on calculations reported in Refs. [50, 52].⁴ At the first stage, we approximated both $C_n(B, T)$ and $C_{\text{MF}}(T)$ by linear functions of the temperature and used also r_{sc} and $T_{c2}(B)$ in Eq. (2) as fit parameters for each magnetic field. At the second stage, we fixed the fit parameters of $C_{\text{MF}}(T)$ and r_{sc} at averaged values for fields from 3 to 9 T, where they change weakly. The best match is achieved for $r_{sc} \approx 177 \text{ K}^{-1/3} \text{ T}^{2/3}$ and $C_{\text{MF}}(T) \approx -183.6 + 6.845T[\text{K}] \text{ kJ/K}\cdot\text{m}^3$ for $31 \text{ K} < T < 35 \text{ K}$. The representative superconducting mean-field and normal backgrounds extracted from this analysis are shown in Fig. 2. As one can see, the procedure leads to the almost perfect collapse of the data to the theoretical scaling curve. We note, however, that the estimate of the parameter r_{sc} from Eq. (3) gives somewhat higher value $\approx 290 \text{ K}^{-1/3} \text{ T}^{2/3}$. The step in the theoretical curve where it features a small discontinuity of $\approx 10\%$ is due to the first-order vortex lattice melting transition, which we discuss below.

Transport measurements show that the resistive transition broadens considerably at finite magnetic fields, see Fig. 2(top). The transition somewhat sharpens when resistivity drops below $\sim 60\%$ of the normal level forming

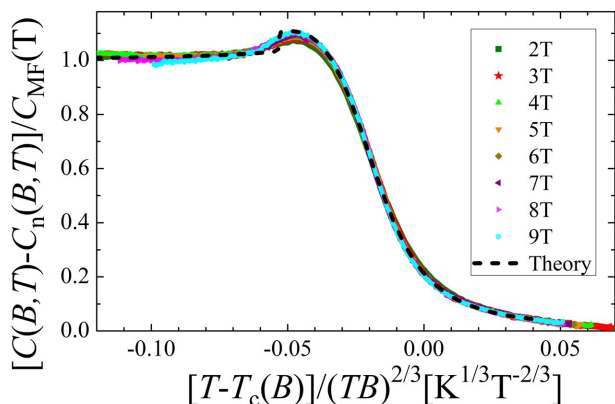


FIG. 3. Scaling plot of the specific heat in the lowest-Landau level regime for high magnetic fields suggested by Eq. (4). The black dashed line is the theoretical LLL scaling function following from calculations in Refs. [50, 52].

⁴ The dominating contribution to the specific-heat scaling function is given by the last term in Eq. (57) of Ref. [50], which is proportional to the second derivative of the free-energy scaling function. The shape of this function plotted in Fig. 3 has been provided to us by the authors of that paper.

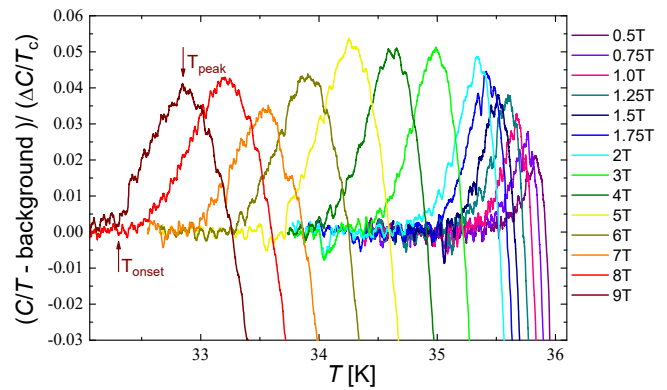


FIG. 4. Steplike feature in the specific heat associated with the vortex melting transition. The curves are obtained by subtracting linear fits for the low-temperature background contribution to enhance the visibility of the melting feature. The onset and peak positions of the step were extracted for the melting line.

a kinklike feature. We interpret this feature as an indication of the first-order-melting resistivity jump smeared by inhomogeneities in the crystal. Similar behavior has been observed in moderately-disordered YBCO samples, while very uniform YBCO crystals feature a very sharp jump. We set the threshold resistance $0.2 \mu\Omega\cdot\text{cm}$ as the criterion for determining the melting temperature in transport measurements. In specific heat, the contribution of the vortex-lattice melting is determined by subtracting from the raw data the linear contribution below the excess-entropy hump. The result, scaled to the jump height at T_c in zero field, $\Delta C/T_c$, is shown in Fig. 4. The relative height of the hump, 4-5% of $\Delta C/T_c$, is in agreement with theoretical expectations for vortex-lattice melting [52]. The spike corresponding to the first-order transition is not visible, probably due to a small number of impurities in the sample. This behavior corresponds to the melting transition broadened by inhomogeneities and it is very similar to Nb_3Sn [7, 32], SnMo_6S_8 [8], and $\text{Ba}_{0.5}\text{K}_{0.5}\text{Fe}_2\text{As}_2$ [42]. In contrast, the specific-heat data in YBCO at high magnetic fields show closer-to-ideal behavior with a pronounced spike at the transition and a distinct step [13]. This difference is not only due to higher homogeneity of the YBCO crystals but also due to much larger Ginzburg-Levanyuk number of this material leading to the large separation between B_m and B_{c2} . Bounds for the melting transition temperature are extracted by evaluating the onset and peak positions of the specific-heat hump, as marked in Fig. 4. The clean-limit melting temperature will lie between these two values. The phase diagram in Fig. 5 shows the melting line extracted from resistivity and calorimetry data, together with the H_{c2} -line extracted from the specific-heat curves by the entropy conserving construction. We also show the theoretical curve obtained using Eq. (8) with the Ginzburg-Levanyuk parameters extracted from the experimental H_{c2} slopes and specific-heat jump at T_c , $\xi_{a0} = 1.46 \text{ nm}$,

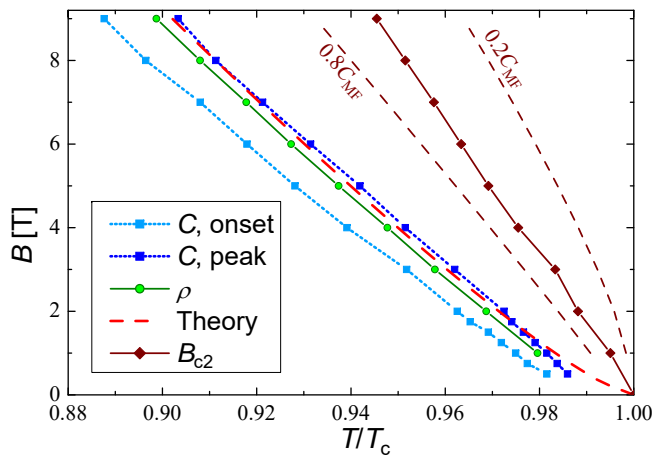


FIG. 5. The vortex melting lines extracted from the specific heat, see Fig. 4, and from vanishing resistivity together with the theoretical curve calculated from Eq. (8). For comparison, we also show the plot of the upper critical field extracted from the specific-heat data. The dashed lines illustrate the fluctuation broadening of the transition and are obtained using the criteria $[C(B, T) - C_n(B, T)]/C_{MF} = 0.2$ and 0.8 .

$\lambda_{ab0} = 98$ nm, and $\gamma = 1.7$. The melting transition line is in excellent agreement with theoretical expectations. We emphasize that the theoretical curve is parameter-free and results purely from the experimental data. We also point out that the location of the melting line is very close to that of a similar compound $Ba_{0.5}K_{0.5}Fe_2As_2$ [42].

To place our results within a broader context, we compare the melting behavior of $RbEuFe_4As_4$ with other superconducting materials. Even though the Ginzburg-Levanyuk number, Eq. (1), is the standard parameter for characterizing thermal fluctuations, it does not directly convey the relative relevance of the thermodynamic phases (liquid and solid) of the vortex matter. Here, we introduce a more intuitive parameter f_{liq} quantifying the fraction of liquid phase in the vortex-matter phase diagram within the Ginzburg-Landau (GL) regime, $T_{GL} < T < T_c$. Here we arbitrarily define the boundary of GL regime as $T_{GL} = 3T_c/4$. Explicitly, this parameter is

$$f_{liq} \equiv \frac{\int_{T_{GL}}^{T_c} (H_{c2} - B_m) dT}{\int_{T_{GL}}^{T_c} H_{c2} dT} = 32 \int_{3/4}^1 (1-t)(1-b_m) dt. \quad (10)$$

We use the interpolation formula in Eq. (9) for its quantitative evaluation. Figure 6 shows the computed dependence $f_{liq}(Gi)$ with points for four representative materials. For weakly-fluctuating materials, in which the melting falls inside the LLL regime, we obtain $f_{liq} \approx 12.8Gi^{1/3} \ll 1$. The liquid phase occupies more than half of the phase space in the GL region already for very small Ginzburg-Levanyuk numbers, $Gi > 6 \cdot 10^{-5}$. $RbEuFe_4As_4$ is only slightly below this threshold and its

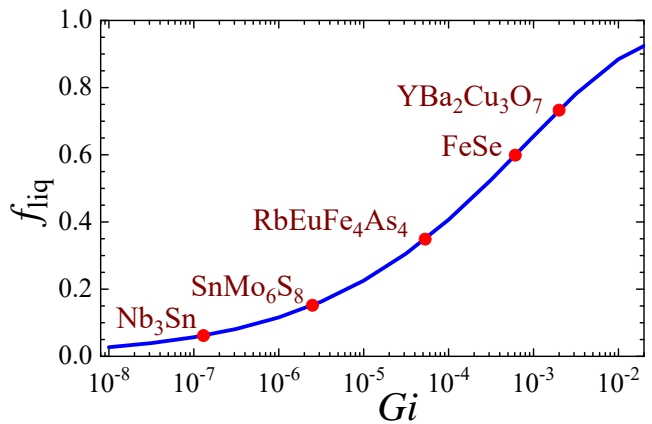


FIG. 6. Dependence of the area fraction occupied by the liquid state, f_{liq} within the GL vortex-matter region ($0.75T_c < T < T_c$, $B < B_{c2}(T)$) on the Ginzburg-Levanyuk number.

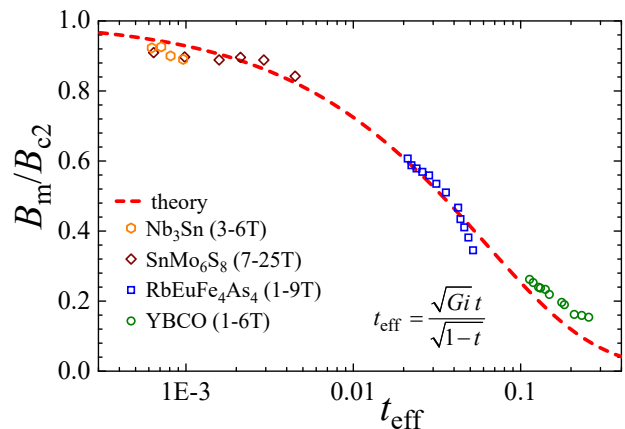


FIG. 7. Universal plot for the vortex-lattice melting transition. The theoretical curve is determined by Eq. (9). The references for used material's data are listed in Table I.

location clearly indicates that, as other iron-based superconductors, this material is in between conventional superconductors and cuprates.

As follows immediately from the form of Eq. (9), the reduced melting field B_m/B_{c2} in the mean-field GL region is a universal function of the effective reduced temperature parameter $t_{eff} = \sqrt{Gi t}/\sqrt{1-t}$ which determines the strength of thermal fluctuations. Figure 7 shows this universal melting plot computed from Eq. (9) together with the points extracted from experimental data for four different materials, Nb_3Sn [7], $SnMo_6S_8$ [8], $RbEuFe_4As_4$ (this work), $YBa_2Cu_3O_7$ [12, 13]. We can see that the experimental melting lines follow the universal trend suggested by theory.

V. SUMMARY

We investigate superconducting thermal fluctuations in single crystals of the magnetic iron-pnictide supercon-

ductor $\text{RbEuFe}_4\text{As}_4$ via transport and calorimetric measurements. We find that the broadening of the specific-heat transition in the magnetic-field range 2-9 T is well described by the lowest-Landau-level scaling. We observe the vortex-lattice melting transition, which is manifested as a steep drop of the resistivity and a step of the specific heat at the field-dependent temperature $T_m(B)$. Melting takes place considerably below the upper critical field. The location of the melting line in the temperature-magnetic field plane is in quantitative agreement with theoretical predictions without fitting parameters. We demonstrate that the reduced melting fields for different materials follow a universal dependence on the effective temperature parameter which determines the strength of thermal fluctuations. Our observations imply that even though thermal fluctuations of vortices are not as prevalent as in HTSC cuprates, they still noticeably influence

the properties of the vortex matter. In particular, we estimate that the liquid phase occupies roughly 40% of the vortex-matter space within the Ginzburg-Landau region.

ACKNOWLEDGMENTS

We would like to thank Dingping Li and Baruch Rosenstein for discussion of the scaling behavior of the specific heat in the LLL regime and providing to us the theoretical scaling function. The work was supported by the US Department of Energy, Office of Science, Basic Energy Sciences, Materials Sciences and Engineering Division. K. W. and R. W. acknowledge support from the Swiss National Science Foundation through the Postdoc Mobility program.

-
- [1] A. A. Abrikosov, On the magnetic properties of superconductors of the second group, [Zh. Eksp. Teor. Fiz. **32**, 1442 (1957)] JETP **5**, 1174 (1957).
- [2] A. Larkin and A. Varlamov, *Theory of Fluctuations in Superconductors*, International Series of Monographs on Physics (Oxford University Press, 2005).
- [3] A. P. Levanyuk, Contribution to the Theory of Light Scattering near the Second-Order Phase-Transition Points, [Zh. Eksp. Teor. Fiz. **36**, 810 (1959)] JETP **9**, 571 (1959).
- [4] V. L. Ginzburg, Some remarks on phase transitions of second kind and the microscopic theory of ferroelectric materials, [Fiz. Tverd. Tela (Leningrad) **2**, 2031 (1960)] Sov. Phys. Solid State **2**, 1824 (1961).
- [5] D. K. Finnemore, T. F. Stromberg, and C. A. Swenson, Superconducting properties of high-purity niobium, Phys. Rev. **149**, 231 (1966).
- [6] J. F. da Silva, E. A. Burgemeister, and Z. Dokoupil, Low temperature specific heat of annealed high-purity niobium in magnetic fields, Physica **41**, 409 (1969).
- [7] R. Lortz, F. Lin, N. Musolino, Y. Wang, A. Junod, B. Rosenstein, and N. Toyota, Thermal fluctuations and vortex melting in the Nb_3Sn superconductor from high resolution specific heat measurements, Phys. Rev. B **74**, 104502 (2006).
- [8] A. P. Petrović, Y. Fasano, R. Lortz, C. Senatore, A. Demuer, A. B. Antunes, A. Paré, D. Salloum, P. Gougeon, M. Potel, and Ø. Fischer, Real-space vortex glass imaging and the vortex phase diagram of SnMo_6S_8 , Phys. Rev. Lett. **103**, 257001 (2009).
- [9] M. P. Smylie, K. Willa, J.-K. Bao, K. Ryan, Z. Islam, H. Claus, Y. Simsek, Z. Diao, A. Rydh, A. E. Koshelev, W.-K. Kwok, D. Y. Chung, M. G. Kanatzidis, and U. Welp, Anisotropic superconductivity and magnetism in single-crystal $\text{RbEuFe}_4\text{As}_4$, Phys. Rev. B **98**, 104503 (2018).
- [10] K. Willa, R. Willa, J.-K. Bao, A. E. Koshelev, D. Y. Chung, M. G. Kanatzidis, W.-K. Kwok, and U. Welp, Strongly fluctuating moments in the high-temperature magnetic superconductor $\text{RbEuFe}_4\text{As}_4$, Phys. Rev. B **99**, 180502 (2019).
- [11] T. Klein and F. Hardy, private communication.
- [12] U. Welp, J. A. Fendrich, W. K. Kwok, G. W. Crabtree, and B. W. Veal, Thermodynamic evidence for a flux line lattice melting transition in $\text{YBa}_2\text{Cu}_3\text{O}_{7-\delta}$, Phys. Rev. Lett. **76**, 4809 (1996).
- [13] A. Schilling, R. A. Fisher, N. E. Phillips, U. Welp, D. Dasgupta, W. K. Kwok, and G. W. Crabtree, Calorimetric measurement of the latent heat of vortex-lattice melting in untwinned $\text{YBa}_2\text{Cu}_3\text{O}_{7-\delta}$, Nature **382**, 791 (1996); A. Schilling, R. A. Fisher, N. E. Phillips, U. Welp, W. K. Kwok, and G. W. Crabtree, Anisotropic latent heat of vortex-lattice melting in untwinned $\text{YBa}_2\text{Cu}_3\text{O}_{7-\delta}$, Phys. Rev. Lett. **78**, 4833 (1997); Angular dependence of the latent heat of vortex-lattice melting in untwinned $\text{YBa}_2\text{Cu}_3\text{O}_{7-\delta}$, Phys. Rev. B **58**, 11157 (1998).
- [14] A. Houghton, R. A. Pelcovits, and A. Sudbø, Flux lattice melting in high- T_c superconductors, Phys. Rev. B **40**, 6763 (1989).
- [15] H. Safar, P. L. Gammel, D. A. Huse, D. J. Bishop, J. P. Rice, and D. M. Ginsberg, Experimental evidence for a first-order vortex-lattice-melting transition in untwinned, single crystal $\text{YBa}_2\text{Cu}_3\text{O}_7$, Phys. Rev. Lett. **69**, 824 (1992).
- [16] W. K. Kwok, S. Fleshler, U. Welp, V. M. Vinokur, J. Downey, G. W. Crabtree, and M. M. Miller, Vortex lattice melting in untwinned and twinned single crystals of $\text{YBa}_2\text{Cu}_3\text{O}_{7-\delta}$, Phys. Rev. Lett. **69**, 3370 (1992).
- [17] M. Charalambous, J. Chaussy, and P. Lejay, Evidence from resistivity measurements along the c axis for a transition within the vortex state for $\text{H}\parallel\text{ab}$ in single-crystal $\text{YBa}_2\text{Cu}_3\text{O}_7$, Phys. Rev. B **45**, 5091 (1992).
- [18] R. Liang, D. A. Bonn, and W. N. Hardy, Discontinuity of reversible magnetization in untwinned YBCO single crystals at the first order vortex melting transition, Phys. Rev. Lett. **76**, 835 (1996).
- [19] T. Nishizaki, Y. Onodera, N. Kobayashi, H. Asaoka, and H. Takei, Magnetization jump and the vortex-lattice melting transition in $\text{YBa}_2\text{Cu}_3\text{O}_y$, Phys. Rev. B **53**, 82 (1996).

- [20] M. Roulin, A. Junod, and E. Walker, Flux line lattice melting transition in $\text{YBa}_2\text{Cu}_3\text{O}_{6.94}$ observed in specific heat experiments, *Science* **273**, 1210 (1996); M. Roulin, A. Junod, A. Erb, and E. Walker, Melting of the flux line lattice observed by specific heat experiments in $\text{YBa}_2\text{Cu}_3\text{O}_{7-\delta}$, *J. Low Temp. Phys.* **105**, 1099 (1996); Calorimetric transitions on the melting line of the vortex system as a function of oxygen deficiency in high-purity $\text{YBa}_2\text{Cu}_3\text{O}_x$, *Phys. Rev. Lett.* **80**, 1722 (1998); B. Revaz, A. Junod, and A. Erb, Specific heat peaks observed up to 16 T on the melting line of vortex matter in $\text{DyBa}_2\text{Cu}_3\text{O}_7$, *Phys. Rev. B* **58**, 11153 (1998).
- [21] F. Bouquet, C. Marcenat, E. Steep, R. Calemczuk, W. K. Kwok, U. Welp, G. W. Crabtree, R. A. Fisher, N. E. Phillips, and A. Schilling, An unusual phase transition to a second liquid vortex phase in the superconductor $\text{YBa}_2\text{Cu}_3\text{O}_7$, *Nature* **411**, 448 (2001).
- [22] B. Khaykovich, E. Zeldov, D. Majer, T. W. Li, P. H. Kes, and M. Konczykowski, Vortex-lattice phase transitions in $\text{Bi}_2\text{Sr}_2\text{CaCu}_2\text{O}_8$ crystals with different oxygen stoichiometry, *Phys. Rev. Lett.* **76**, 2555 (1996).
- [23] S. Ooi, T. Shibauchi, and T. Tamegai, Evolution of vortex phase diagram with oxygen-doping in $\text{Bi}_2\text{Sr}_2\text{CaCu}_2\text{O}_{8+y}$ single crystals, *Physica C* **302**, 339 (1998).
- [24] H. Beidenkopf, T. Verdene, Y. Myasoedov, H. Shtrikman, E. Zeldov, B. Rosenstein, D. Li, and T. Tamegai, Interplay of anisotropy and disorder in the doping-dependent melting and glass transitions of vortices in $\text{Bi}_2\text{Sr}_2\text{CaCu}_2\text{O}_{8+\delta}$, *Phys. Rev. Lett.* **98**, 167004 (2007).
- [25] R. Cubitt, E. M. Forgan, G. Yang, S. L. Lee, D. M. Paul, H. A. Mook, M. Yethiraj, P. H. Kes, T. W. Li, A. A. Menovsky, Z. Tarnawski, and K. Mortensen, Direct observation of magnetic flux lattice melting and decomposition in the high- T_c superconductor $\text{Bi}_{2.15}\text{Sr}_{1.95}\text{CaCu}_2\text{O}_{8+x}$, *Nature* **365**, 407 (1993).
- [26] S. L. Lee, P. Zimmermann, H. Keller, M. Warden, I. M. Savić, R. Schauwecker, D. Zech, R. Cubitt, E. M. Forgan, P. H. Kes, T. W. Li, A. A. Menovsky, and Z. Tarnawski, Evidence for flux-lattice melting and a dimensional crossover in single-crystal $\text{Bi}_{2.15}\text{Sr}_{1.85}\text{CaCu}_2\text{O}_{8+\delta}$ from muon spin rotation studies, *Phys. Rev. Lett.* **71**, 3862 (1993).
- [27] A. Oral, J. C. Barnard, S. J. Bending, I. I. Kaya, S. Ooi, T. Tamegai, and M. Henini, Direct observation of melting of the vortex solid in $\text{Bi}_2\text{Sr}_2\text{CaCu}_2\text{O}_{8+\delta}$ single crystals, *Phys. Rev. Lett.* **80**, 3610 (1998).
- [28] H. Pastoriza, M. F. Goffman, A. Arribère, and F. de la Cruz, First order phase transition at the irreversibility line of $\text{Bi}_2\text{Sr}_2\text{CaCu}_2\text{O}_8$, *Phys. Rev. Lett.* **72**, 2951 (1994).
- [29] E. Zeldov, D. Majer, M. Konczykowski, V. B. Geshkenbein, V. M. Vinokur, and H. Shtrikman, Thermodynamic observation of first-order vortex-lattice melting transition in $\text{Bi}_2\text{Sr}_2\text{CaCu}_2\text{O}_8$, *Nature* **375**, 373 (1995); D. T. Fuchs, E. Zeldov, D. Majer, R. A. Doyle, T. Tamegai, S. Ooi, and M. Konczykowski, Simultaneous resistivity onset and first-order vortex-lattice phase transition in $\text{Bi}_2\text{Sr}_2\text{CaCu}_2\text{O}_8$, *Phys. Rev. B* **54**, R796 (1996).
- [30] D. E. Farrell, E. Johnston-Halperin, L. Klein, P. Fournier, A. Kapitulnik, E. M. Forgan, A. I. M. Rae, T. W. Li, M. L. Trawick, R. Sasik, and J. C. Garland, Magnetization jumps and irreversibility in $\text{Bi}_2\text{Sr}_2\text{CaCu}_2\text{O}_8$, *Phys. Rev. B* **53**, 11807 (1996).
- [31] T. Sasagawa, K. Kishio, Y. Togawa, J. Shimoyama, and K. Kitazawa, First-order vortex-lattice phase transition in $(\text{La}_{1-x}\text{Sr}_x)_2\text{CuO}_4$ single crystals: Universal scaling of the transition lines in high-temperature superconductors, *Phys. Rev. Lett.* **80**, 4297 (1998).
- [32] R. Lortz, N. Musolino, Y. Wang, A. Junod, and N. Toyota, Origin of the magnetization peak effect in the Nb_3Sn superconductor, *Phys. Rev. B* **75**, 094503 (2007).
- [33] J. Paglione and R. L. Greene, High-temperature superconductivity in iron-based materials, *Nat. Phys.* **6**, 645 (2010).
- [34] G. R. Stewart, Superconductivity in iron compounds, *Rev. Mod. Phys.* **83**, 1589 (2011).
- [35] H. Hosono and K. Kuroki, Iron-based superconductors: Current status of materials and pairing mechanism, *Physica C* **514**, 399 (2015).
- [36] A. Iyo, K. Kawashima, T. Kinjo, T. Nishio, S. Ishida, H. Fujihisa, Y. Gotoh, K. Kihou, H. Eisaki, and Y. Yoshida, New-structure-type Fe-based superconductors: $\text{CaAFe}_4\text{As}_4$ ($A = \text{K, Rb, Cs}$) and $\text{SrAFe}_4\text{As}_4$ ($A = \text{Rb, Cs}$), *J. Am. Chem. Soc.* **138**, 3410 (2016).
- [37] H. Q. Yuan, J. Singleton, F. F. Balakirev, S. A. Baily, G. F. Chen, J. L. Luo, and N. L. Wang, Nearly isotropic superconductivity in $(\text{Ba,K})\text{Fe}_2\text{As}_2$, *Nature* **457**, 565 (2009).
- [38] U. Welp, R. Xie, A. E. Koshelev, W. K. Kwok, H. Q. Luo, Z. S. Wang, G. Mu, and H. H. Wen, Anisotropic phase diagram and strong coupling effects in $\text{Ba}_{1-x}\text{K}_x\text{Fe}_2\text{As}_2$ from specific-heat measurements, *Phys. Rev. B* **79**, 094505 (2009).
- [39] D. L. Sun, Y. Liu, and C. T. Lin, Comparative study of upper critical field H_{c2} and second magnetization peak H_{sp} in hole- and electron-doped BaFe_2As_2 superconductor, *Phys. Rev. B* **80**, 144515 (2009).
- [40] C. Tarantini, A. Gurevich, J. Jaroszynski, F. Balakirev, E. Bellingeri, I. Pallecchi, C. Ferdeghini, B. Shen, H. H. Wen, and D. C. Larbalestier, Significant enhancement of upper critical fields by doping and strain in iron-based superconductors, *Phys. Rev. B* **84**, 184522 (2011).
- [41] J. Mosqueira, J. D. Dancausa, F. Vidal, S. Salem-Sugui, A. D. Alvarenga, H.-Q. Luo, Z.-S. Wang, and H.-H. Wen, Observation of anisotropic diamagnetism above the superconducting transition in iron pnictide $\text{Ba}_{1-x}\text{K}_x\text{Fe}_2\text{As}_2$ single crystals due to thermodynamic fluctuations, *Phys. Rev. B* **83**, 094519 (2011); S. Salem-Sugui, L. Ghivelder, A. D. Alvarenga, J. L. Pimentel, H. Luo, Z. Wang, and H.-H. Wen, Superconducting fluctuations in the reversible magnetization of the iron-pnictide $\text{Ba}_{1-x}\text{K}_x\text{Fe}_2\text{As}_2$, *Phys. Rev. B* **80**, 014518 (2009); A. Ramos-Álvarez, J. Mosqueira, F. Vidal, D. Hu, G. Chen, H. Luo, and S. Li, Superconducting fluctuations in isovalently substituted $\text{BaFe}_2(\text{As}_{1-x}\text{P}_x)_2$: Possible observation of multiband effects, *Phys. Rev. B* **92**, 094508 (2015).
- [42] H. K. Mak, P. Burger, L. Cevey, T. Wolf, C. Meingast, and R. Lortz, Thermodynamic observation of a vortex melting transition in the Fe-based superconductor $\text{Ba}_{0.5}\text{K}_{0.5}\text{Fe}_2\text{As}_2$, *Phys. Rev. B* **87**, 214523 (2013).
- [43] Y. Liu, Y.-B. Liu, Z.-T. Tang, H. Jiang, Z.-C. Wang, A. Ablimit, W.-H. Jiao, Q. Tao, C.-M. Feng, Z.-A. Xu, and G.-H. Cao, Superconductivity and ferromagnetism in hole-doped $\text{RbEuFe}_4\text{As}_4$, *Phys. Rev. B* **93**, 214503 (2016).
- [44] J.-K. Bao, K. Willa, M. P. Smylie, H. Chen, U. Welp, D. Y. Chung, and M. G. Kanatzidis, Single crystal growth and study of the ferromagnetic superconductor

- RbEuFe₄As₄, *Crystal Growth & Design*, Crystal Growth & Design **18**, 3517 (2018).
- [45] V. S. Stolyarov, A. Casano, M. A. Belyanchikov, A. S. Astrakhantseva, S. Y. Grebenchuk, D. S. Baranov, I. A. Golovchanskiy, I. Voloshenko, E. S. Zhukova, B. P. Gorshunov, A. V. Muratov, V. V. Dremov, L. Y. Vinnikov, D. Roditchev, Y. Liu, G.-H. Cao, M. Dressel, and E. Uykur, Unique interplay between superconducting and ferromagnetic orders in EuRbFe₄As₄, *Phys. Rev. B* **98**, 140506 (2018).
- [46] D. E. Jackson, D. VanGennep, W. Bi, D. Zhang, P. Materne, Y. Liu, G.-H. Cao, S. T. Weir, Y. K. Vohra, and J. J. Hamlin, Superconducting and magnetic phase diagram of RbEuFe₄As₄ and CsEuFe₄As₄ at high pressure, *Phys. Rev. B* **98**, 014518 (2018).
- [47] D. J. Thouless, Critical fluctuations of a type-II superconductor in a magnetic field, *Phys. Rev. Lett.* **34**, 946 (1975).
- [48] E. Brézin, A. Fujita, and S. Hikami, Large-order behavior of the perturbation series for superconductors near H_{c2} , *Phys. Rev. Lett.* **65**, 1949 (1990).
- [49] Z. Tešanović and A. V. Andreev, Thermodynamic scaling functions in the critical region of type-II superconductors, *Phys. Rev. B* **49**, 4064 (1994).
- [50] D. Li and B. Rosenstein, Supercooled vortex liquid and quantitative theory of melting of the flux-line lattice in type-II superconductors, *Phys. Rev. B* **70**, 144521 (2004).
- [51] B. Rosenstein and D. Li, Ginzburg-Landau theory of type II superconductors in magnetic field, *Rev. Mod. Phys.* **82**, 109 (2010).
- [52] D. Li and B. Rosenstein, Melting of the vortex lattice in high- T_c superconductors, *Phys. Rev. B* **65**, 220504 (2002).
- [53] R. Šášik and D. Stroud, First-order vortex lattice melting and magnetization of YBa₂Cu₃O_{7- δ} , *Phys. Rev. Lett.* **75**, 2582 (1995); J. Hu and A. H. MacDonald, Universal phase diagram for vortex states of layered superconductors in strong magnetic fields, *Phys. Rev. B* **56**, 2788 (1997).
- [54] H. Nordborg and G. Blatter, Numerical study of vortex matter using the Bose model: First-order melting and entanglement, *Phys. Rev. B* **58**, 14556 (1998).
- [55] T. Chen and S. Teitel, Phase transitions in high- T_c superconductors and the anisotropic three-dimensional XY model, *Phys. Rev. B* **55**, 11766 (1997); A. E. Koshelev, Point-like and line-like melting of the vortex lattice in the universal phase diagram of layered superconductors, *Phys. Rev. B* **56**, 11201 (1997).
- [56] A. E. Koshelev and H. Nordborg, Universal properties for linelike melting of the vortex lattice, *Phys. Rev. B* **59**, 4358 (1999).
- [57] S. Tagliati, V. M. Krasnov, and A. Rydh, Differential membrane-based nanocalorimeter for high-resolution measurements of low-temperature specific heat, *Rev. Sci. Instrum.* **83**, 055107 (2012).
- [58] K. Willa, Z. Diao, D. Campanini, U. Welp, R. Divan, M. Hudl, Z. Islam, W.-K. Kwok, and A. Rydh, Nanocalorimeter platform for in situ specific heat measurements and x-ray diffraction at low temperature, *Rev. Sci. Instrum.* **88**, 125108 (2017).